Int. J Multiphase Flow Vol 12, No 4, pp 505–529, 1986
Printed in Great Britain

0301-9322/86 $3.00+.00
Pergamon Journals/Elsevier

LOCAL FORMULATION AND MEASUREMENTS OF INTERFACIAL AREA CONCENTRATION IN TWO-PHASE FLOW

ISAO KATAOKA
Institute of Atomic Energy, Kyoto University, Uji, Kyoto 611, Japan

MAMORU ISHII†
Reactor Analysis and Safety Division, Argonne National Laboratory, Argonne, IL 60439, U.S.A.

and

AKIMI SERIZAWA
Department of Nuclear Engineering, Kyoto University, Sakyo-ku, Kyoto 606, Japan

(*Received* 20 *February* 1985, *in revised form* 22 *August* 1985)

Abstract—The interfacial area concentration is one of the most important parameters in analyzing two-phase flow based on the two-fluid model. The local instantaneous formulation of the interfacial area concentration is introduced here. Based on this formulation, time and spatial averaged interfacial area concentrations are derived, and the local ergodic theorem (the equivalency of the time and spatial averaged values) is obtained for stationary developed two-phase flow. On the other hand, the global ergodic theorem is derived for general two-phase flow. Measurement methods are discussed in detail in relation to the present analysis. The three-probe method, with which local interfacial area concentration can be measured accurately, has been proposed. The one-probe method under some statistical assumptions has also been proposed. In collaboration with the experimental data for the interfacial velocity, radial profiles of the local interfacial area concentration are obtained based on the one-probe method. The result indicates that the local interfacial area concentration has a peak value near the tube wall in bubbly flow. This is consistent with the near wall peak of local void fraction separately observed. In slug flow it shows a higher value in the central region of the tube for that particular set of data

1. INTRODUCTION

In order to analyze the thermal hydraulics of two-phase flow, various formulations such as the homogeneous flow model, drift-flux model (Zuber & Findley 1965; Wallis 1969; Ishii 1977), and two-fluid model have been proposed (Ishii 1975; Delhaye 1968). Among these models, the two-fluid formulation can be considered the most accurate model because of its detailed treatment of the phase interactions at the interface. The two-fluid model is formulated by considering each phase separately in terms of two sets of conservation equations which govern the balance of mass, momentum, and energy of each phase. These balance equations represent the macroscopic fields of each phase and are obtained from proper averaging methods. Since the macroscopic fields of each phase are not independent of the other phase, the phase interaction terms which couple the transport of mass, momentum, and energy of each phase appear in the field equations. It is expected that the two-fluid model can predict mechanical and thermal nonequilibrium between phases accurately. However, it is noted that the interfacial transfer terms should be modeled accurately for the two-fluid model to be useful. In the present state of the art, the constitutive equations for these interfacial terms are the weakest link in the two-fluid model. The difficulties arise due to the complicated transfer mechanisms at the interfaces coupled with the motion and geometry of the interfaces. Furthermore, the constitutive equations should be modeled by macroscopic variables based on proper averaging. A three-dimensional two-fluid model has been obtained by using temporal or statistical averaging (Ishii 1975). For most practical

† Author to whom correspondence should be addressed.

applications, the model developed by Ishii (1975) can be simplified to the following forms

Continuity equation

$$\frac{\partial \alpha_k \rho_k}{\partial t} + \nabla \cdot (\alpha_k \rho_k \mathbf{v}_k) = \Gamma_k ; \quad [1]$$

Momentum equation

$$\frac{\partial \alpha_k \rho_k \mathbf{v}_k}{\partial t} + \nabla \cdot (\alpha_k \rho_k \mathbf{v}_k \mathbf{v}_k) = -\alpha_k \nabla p_k + \nabla \cdot \alpha_k (\bar{\bar{\tau}}_k + \tau_k^t) + \alpha_k \rho_k \mathbf{g} + \mathbf{v}_{ki} \Gamma_k + \mathbf{M}_{ik} - \nabla \alpha_k \cdot \tau_i . \quad [2]$$

Enthalpy energy equation

$$\frac{\partial \alpha_k \rho_k H_k}{\partial t} + \nabla \cdot (\alpha_k \rho_k H_k \mathbf{v}_k) = -\nabla \cdot \alpha_k (\bar{\bar{q}}_k + q_k^t) + \alpha_k \frac{D_k}{Dt} p_k + H_{ki} \Gamma_k + \frac{q_{ki}''}{L_s} + \Phi_k \quad [3]$$

Here Γ_k, $\mathbf{M}_{ik}$, τ_i, q_{ki}'', and Φ_k are the mass generation, generalized interfacial drag, interfacial shear stress, interfacial heat flux, and dissipation, respectively. The subscript k denotes k phase, and i stands for the value at the interface. α_k, ρ_k, $\mathbf{v}_k$, p_k, and H_k denote the void fraction, density, velocity, pressure and enthalpy of k phase, whereas $\bar{\bar{\tau}}_k$, τ_k^t, $\bar{\bar{q}}_k$, q_k^t, and $\mathbf{g}$ stand for average viscous stress, turbulent stress, mean conduction heat flux, turbulent heat flux and acceleration due to gravity. H_{ki} is the enthalpy of k phase at the interface; thus it may be assumed to be the saturation enthalpy for most cases. L_s denotes the length scale at the interface, and $1/L_s$ has the physical meaning of the interfacial area per unit volume a_i (Ishii 1975). Thus,

$$\frac{1}{L_s} = a_i = \frac{\text{Interfacial area}}{\text{Mixture volume}} . \quad [4]$$

The above field equations indicate that several interfacial transfer terms appear on the right-hand sides of the equations. Since these interfacial transfer terms also should obey the balance laws at the interface, interfacial transfer conditions could be obtained from an average of the local jump conditions (Ishii 1975). They are given by

$$\sum_k \Gamma_k = 0 , \quad \sum_k \mathbf{M}_{ik} = 0 , \quad \sum_k \left(\Gamma_k H_{ki} + \frac{q_{ki}''}{L_s} \right) = 0 . \quad [5]$$

Therefore, constitutive equations for $\mathbf{M}_{ik}$, q_{Gi}''/L_s, and q_{Li}''/L_s are necessary for the interfacial transfer terms. The enthalpy interfacial transfer condition indicates that specifying the heat flux at the interface for both phases is equivalent to the constitutive relation for Γ_k if the mechanical-energy transfer terms can be neglected (Ishii 1975). This aspect greatly simplifies the development of the constitutive relations for interfacial transfer terms.

By introducing the mean mass transfer per unit area, m_k, defined by

$$\Gamma_k \equiv a_i m_k , \quad [6]$$

the interfacial energy-transfer term in [3] can be rewritten as

$$\Gamma_k H_{ki} + \frac{q''_{ki}}{L_s} = a_i(m_k H_{ki} + q''_{ki}) . \quad [7]$$

The heat flux at the interface should be modeled using the driving force or the potential for an energy transfer. Thus,

$$q''_{ki} = h_{ki}(T_i - T_k) , \quad [8]$$

where T_i and T_k are the interfacial and bulk temperatures based on the mean enthalpy and h_{ki} is the interfacial heat transfer coefficient. A similar treatment of the interfacial momentum transfer term is also possible (Ishii & Mishima 1980). In view of the above, the importance of the interfacial area a_i, in developing a constitutive relation for this term is evident. The interfacial transfer terms are now expressed as a product of the interfacial area and the driving force. It is essential to make a conceptual distinction between the effects of these two parameters. The interfacial transfer of mass, momentum, and energy increases with an interfacial area concentration toward the mechanical and thermal equilibrium.

Thus, in general, the interfacial transfer terms are given in terms of the interfacial area concentration a_i and driving force (Ishii 1975; Ishii & Mishima 1980; Ishii *et al.* 1982) as

$$\text{(Interfacial transfer term)} \sim a_i \times \text{(Driving force)} . \quad [9]$$

The area concentration defined as the interfacial area per unit volume of the mixture characterizes the first-order geometrical effects; therefore, it must be related to the structure of the two-phase flow field. On the other hand, the driving forces for the interfacial transport characterize the local transport mechanisms such as the turbulent and molecular diffusions.

In two-phase flow systems, the void fraction and interfacial area concentration are two of the most important geometrical parameters. The void fraction is treated as a variable to be solved from a set of balance equations, whereas the interfacial area concentration should be specified by a constitutive relation or by introducing an additional transport equation for a_i (Ishii 1975; Ishii & Mishima 1980). As the above formulation indicates, the knowledge of the interfacial area concentration is indispensable in the two-fluid model.

Although a number of studies have been made in this area, the interfacial area concentration in two-phase flow has not been sufficiently investigated both experimentally and analytically. Most of the previous studies are for steady-state flow without phase change. Available experimental data are limited to volume-averaged interfacial area concentration over a section of a flow channel. Detailed review of these are given in references (Ishii & Mishima 1980) to (Kocamustafaogullari & Ishii 1983). There are a number of shortcomings in measurement techniques. Furthermore, there are very few established theoretical foundations for relating this interfacial area to some easily measurable quantities. In particular, there seems to be no information available on a local value of the interfacial area concentration. However, this local interfacial area concentration is very important for two- or three-dimensional analyses using the two-fluid model.

There is one problem dealing with the definition of the interfacial area concentration locally and instantaneously. Since the Lebesque measure of an interface is zero, the local instantaneous interfacial area concentration cannot be represented by an ordinary function (Schwartz 1950; 1951; 1961). To avoid this problem, an integral method has been used in the analysis of the interfacial area (Ishii 1975; Delhaye 1968). However, by introducing a distribution which is a generalized function (Schwartz 1950; 1951; 1961), one can express the local instantaneous interfacial area concentration.

Based on this local instantaneous formulation and the assumptions of the statistical characteristics of two-phase flow, fundamental relations for the interfacial area concentration have been derived. These equations relate the local value of the interfacial area to observable parameters of the two-phase flow. Based on this theory, some measurement techniques of

the local interfacial area concentration have been proposed. Finally, using the existing experimental data on flow measurements, radial profiles of the local interfacial concentration have been obtained.

2 LOCAL INSTANTANEOUS INTERFACIAL AREA CONCENTRATION

By considering a simple system shown in figure 1, where there is only one gas–liquid interface, the location of the interface x_0 is represented in an x coordinate as

$$x = x_0 \qquad [10]$$

Now a control volume near the point γ is defined by

$$\gamma - \frac{1}{2}\Delta x \leqslant x \leqslant \gamma + \frac{1}{2}\Delta x\,, \qquad [11]$$

where Δx is the size of the control volume. Then the spatial-averaged interfacial area concentration $\bar{a}_i^p$ in the control volume is given by

$$\begin{aligned} \bar{a}_i^p &= \frac{1}{\Delta x} \quad \text{for } |\gamma - x_0| < \frac{\Delta x}{2}\,, \\ &= 0 \quad \text{for } |\gamma - x_0| > \frac{\Delta x}{2}\,. \end{aligned} \qquad [12]$$

By taking the limit of $\Delta x \to 0$, the local interfacial area concentration $a_i(x)$ in a one-dimensional form is given by

$$a_i(x) = \delta(x - x_0)\,. \qquad [13]$$

Here $\delta(x - x_0)$ is the delta function (Dirac 1958; Schwartz 1961) which satisfies

$$\int_{-\infty}^{\infty} \delta(x - x_0)\mathrm{d}x = 1\,, \quad \delta(x - x_0) = 0 \text{ for } x \neq x_0\,. \qquad [14]$$

One of the special characteristics of the delta function is that for any smooth function $\phi(x)$ it gives

$$\int_{-\infty}^{\infty} \delta(x - x_0)\,\phi(x)\mathrm{d}x = \phi(x_0)\,. \qquad [15]$$

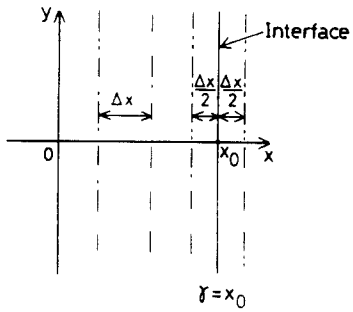

Figure 1 Local interfacial area concentration in one dimension

This result can be extended to any gas–liquid interface in a three-dimensional space. By considering a moving gas–liquid interface which is smooth and represented by

$$f(x,y,z,t) = 0\,, \qquad [16]$$

the local instantaneous interacial area concentration a_i is given by

$$a_i(x,y,z,t) = |\mathbf{grad}\ f|\ \delta(f(x,y,z,t))\,, \qquad [17]$$

where $|\mathbf{grad}\ f|$ is defined as

$$|\mathbf{grad}\ f| = \sqrt{\mathbf{grad}\ f \cdot \mathbf{grad}\ f} = \sqrt{\left(\frac{\partial f}{\partial x}\right)^2 + \left(\frac{\partial f}{\partial y}\right)^2 + \left(\frac{\partial f}{\partial z}\right)^2}\,. \qquad [18]$$

In bubbly or droplet flow, the gas–liquid interface is composed of many separate surfaces of bubbles or droplets. For this case, the surface of the jth bubble or droplet is represented by

$$f_j(x,y,z,t) = 0\,. \qquad [19]$$

Then the local instantaneous interfacial area concentration is given by

$$a_i(x,y,z,t) = \sum_j |\mathbf{grad}\ f_j|\ \delta(f_j(x,y,z,t))\,. \qquad [20]$$

The above analysis shows that the local instantaneous formulations of interfacial area concentration can be obtained in terms of a distribution, as in [20]. This formulation is valid for any flow regime of two-phase flow.

Since the distribution $\delta(x - x_0)$ is not observable experimentally, it is necessary to apply appropriate averaging of [17] or [20] to obtain a measurable representation of the interfacial area concentration. Time and spatial averaging will be discussed in this relation in the next section.

A. Spatial averaging of interfacial area

In general, there are three types of spatial averaging of $a_i(x,y,z,t)$, which are linear, surface, and volume averaging.

Now, in view of its practical importance for the present study, the linear averaging $\bar{a}_i^{pz}$ along the z axis is discussed in detail. For fixed x_0, y_0, and t_0, the spatial average of [20] over length L is given by

$$\begin{aligned}\bar{a}_i^{pz}(x_0,y_0,t_0) &= \frac{1}{L}\int_z^{z+L} a_i(x_0,y_0,z,t_0)\mathrm{d}z \\ &= \frac{1}{L}\sum_j \int_z^{z+L} |\mathbf{grad}\ f_j|\ \delta(f_j(x_0,y_0,z,t_0))\mathrm{d}z\,.\end{aligned} \qquad [21]$$

By defining z_j as the value which satisfies

$$f_j(x_0,y_0,z_j,t_0) = 0\,, \qquad [22]$$

[21] can be rewritten as

$$\bar{a}_i^{pz}(x_0,y_0,t_0) = \frac{1}{L}\sum_j \left\{|\mathbf{grad}\ f_j| \Big/ \left|\frac{\partial f_j}{\partial z}\right|\right\}\,. \qquad [23]$$

Here the right-hand side is calculated at (x_0,y_0,z_j,t_0) and for jth interface satisfying $z < z_j < z + L$. By denoting the angle between the z axis and the direction of the jth surface normal vector at (x_0,y_0,z_j,t_0) as θ_j (see figure 2), it can be shown that

$$\cos\ \theta_j = \left|\frac{\partial f_j}{\partial z}\right| / |\mathbf{grad}\ f_j| . \qquad [24]$$

Therefore, [23] becomes

$$\bar{a}_i^{pz}(x_0,y_0,t_0) = \frac{1}{L}\sum_j \frac{1}{\cos\ \theta_j} = \frac{(\Sigma)_j}{L}\left\{\sum_j \frac{1}{\cos\ \theta_j} \Big/ \left(\sum_j\right)\right\}, \qquad [25]$$

where $(\Sigma)_j$ denotes the number of interfaces within the domain. Here j is arranged such that z_j is in increasing order,

$$z < \cdots z_{j-1} < z_j < z_{j+1} \cdots < z + L \qquad [26]$$

Furthermore, it is assumed that the following uniformity of the two-phase flow exists in the z direction for a reasonably large number of samples, where l is the average distance between interfaces in the z direction:

$$\lim_{n\to\infty} \frac{1}{2n+1} \sum_{j=-n}^{n} |z_{j+1} - z_j| = l \qquad [27]$$

Then it can be shown that for large L,

$$\left(\sum_j\right) = \frac{L}{l} . \qquad [28]$$

Substituting [28] into [25], one finally obtains

$$\bar{a}_i^{pz}(x_0,y_0,t_0) = \frac{1}{l}\overline{\frac{1}{\cos\ \theta}} . \qquad [29]$$

Here $\overline{(1/\cos\ \theta)}$ is the reciprocal of a harmonic mean of $\cos\ \theta_j$ given by

$$\overline{\frac{1}{\cos\ \theta}} = \left\{\sum_j \frac{1}{\cos\ \theta_j}\right\} \Big/ \left(\sum_j\right) . \qquad [30]$$

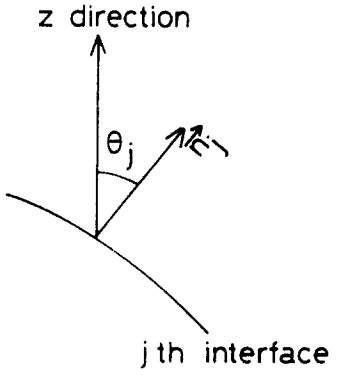

Figure 2 Angle between $\mathbf{n}_z$ (z direction) and $\mathbf{n}_j$

On the other hand, by denoting the number of bubbles or droplets per unit length of z axis by N_z, l can be given by

$$l = \frac{1}{2N_z}. \qquad [31]$$

Here the factor 2 indicates that bubble or droplet has two interfaces (upper and lower) in the z direction. Then [29] can be rewritten as

$$\bar{a}_i^{pz}(x_0,y_0,t_0) = 2N_z \overline{\frac{1}{\cos\theta}}. \qquad [32]$$

Equation [32] implies that the interfacial area concentration can be obtained by measuring the number of bubbles or droplets per unit length and the harmonic average of cos θ_j along z direction.

B. Time averaging of interfacial area

For fixed x_0, y_0, and z_0, the time averaging of [20] over interval Ω is given in terms of the time-averaged area concentration $\bar{a}_i^t$ as

$$\bar{a}_i^t(x_0,y_0,z_0) = \frac{1}{\Omega}\int_t^{t+\Omega} a_i(x_0,y_0,z_0,t)\mathrm{d}t = \frac{1}{\Omega}\sum_j \int_t^{t+\Omega} |\mathbf{grad}\ f_j|\,\delta(f_j)\mathrm{d}t. \qquad [33]$$

Now t_j is defined as the time which satisfies

$$f_j(x_0,y_0,z_0,t_j) = 0. \qquad [34]$$

Then [33] can be rewritten as

$$\bar{a}_i^t(x_0,y_0,z_0) = \frac{1}{\Omega}\sum_j \left\{ |\mathbf{grad}\ f_j| \Big/ \left|\frac{\partial f_j}{\partial t}\right| \right\} \text{ at } (x_0,y_0,z_0,t_j), \qquad [35]$$

which applies for j satisfying $t < t_j < t + \Omega$.

By defining ϕ_j as the angle between the velocity of the jth interface, $\mathbf{v}_{ij}$, and the direction of the surface normal vector at (x_0,y_0,z_0,t_j) (see figure 3), the following relation can be obtained.

$$|\mathbf{grad}\ f_j| \Big/ \left|\frac{\partial f_j}{\partial t}\right| = \frac{1}{|\mathbf{v}_{ij}|\cos\phi_j}. \qquad [36]$$

Substituting [36] into [35], one gets

$$\bar{a}_i^t(x_0,y_0,z_0) = \frac{1}{\Omega}\sum_j \frac{1}{|\mathbf{v}_{ij}|\cos\phi_j} = \frac{(\Sigma)_j}{\Omega} \cdot \left\{ \left(\sum_j \frac{1}{|\mathbf{v}_{ij}|\cos\phi_j}\right) \Big/ \left(\sum_j\right) \right\} \qquad [37]$$

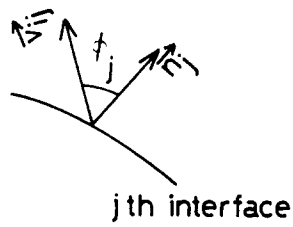

Figure 3. Angle between $\mathbf{v}_{ij}$ and $\mathbf{n}_j$.

for all j satisfying $t < t_j < t + \Omega$. The above result has been obtained also by Ishii (1975) and Delhaye (1976; 1980) using the integral method.

Now j is rearranged so that t_j is in increasing order as

$$\cdots < t_{j-1} < t_j < t_{j+1} < t_{j+2} < \cdots . \qquad [38]$$

Then by assuming the following uniformity of the time intervals with mean value τ

$$\lim_{n\to\infty} \frac{1}{2n+1} \sum_{j=-n}^{n} |t_{j+1} - t_j| = \tau , \qquad [39]$$

one obtains the following relation for large Ω,

$$\left(\sum_j\right) = \frac{\Omega}{\tau} . \qquad [40]$$

Substituting [40] into [37] yields

$$\bar{a}_i^t (x_0,y_0,z_0) = \frac{1}{\tau} \overline{\frac{1}{|\mathbf{v}_i|\cos\ \phi}} . \qquad [41]$$

Here the reciprocal of a harmonic mean of $|\mathbf{v}_{ij}|\cos\ \phi_j$ is given by

$$\overline{\frac{1}{|\mathbf{v}_i|\cos\ \phi}} = \sum_j \frac{1}{|\mathbf{v}_{ij}|\cos\ \phi_j} \Big/ \left(\sum_j\right) . \qquad [42]$$

Now if the number of bubbles or droplets which pass the point (x_0,y_0,z_0) per unit time is denoted by N_t, then τ can be given by

$$\tau = \frac{1}{2N_t} . \qquad [43]$$

Here the factor 2 indicates that one bubble or droplet passing (x_0,y_0,z_0) has two interfaces associated with it. Thus, [41] can be rewritten as

$$\bar{a}_i^t (x_0,y_0,z_0) = 2N_t \overline{\frac{1}{|\mathbf{v}_i|\cos\ \phi}} . \qquad [44]$$

This equation indicates that the time-averaged interfacial area concentration can be obtained by counting N_t and knowing $|\mathbf{v}_{ij}|\cos\ \phi_j$ for each interface.

If one assumes that $1/|\mathbf{v}_{ij}|$ and $1/\cos\ \phi_j$ have no correlation, one obtains

$$\bar{a}_i^t (x_0,y_0,z_0) = 2N_t \overline{\frac{1}{|\mathbf{v}_i|}} \cdot \overline{\frac{1}{\cos\ \phi}} , \qquad [45]$$

where

$$\overline{\frac{1}{|\mathbf{v}_i|}} = \sum_j \frac{1}{|\mathbf{v}_{ij}|} \Big/ \left(\sum_j\right) \qquad [46]$$

and

$$\overline{\frac{1}{\cos\ \phi}} = \sum_j \frac{1}{\cos\ \phi_j} \Big/ \left(\sum_j\right) . \qquad [47]$$

C. Ergodic hypothesis of interfacial area concentration

In the previous sections, spatial and time averaging of the interfacial area concentration has been discussed. However, there is one interesting and particularly important problem to consider. This is related to the ergodic hypothesis. It is essential to know under what conditions the time and spatial averages coincide. A general answer to this problem is quite difficult to obtain and beyond the scope of this paper. However, for stationary and developed two-phase flow this ergodic hypothesis can be demonstrated as shown below.

First, the integration of $a_i(x,y,z,t)$ in volume domain V and time domain Ω is considered. This is denoted by $I(V,\Omega)$ and given by

$$I(V,\Omega) = \int\int\int\int_{V,\Omega} a_i(x,y,z,t)\mathrm{d}x\ \mathrm{d}y\ \mathrm{d}z\ \mathrm{d}t\,. \qquad [48]$$

This integral represents the total area of interface in the volume domain V and over the time interval Ω. The sequential integration in time domain Ω and volume V coincides with $I(V,\Omega)$; thus,

$$\int\int\int_V \left[\int_\Omega a_i(x,y,z,t)dt\right]\mathrm{d}x\ \mathrm{d}y\ \mathrm{d}z = \int_\Omega \left[\int\int\int_V a_i(x,y,z,t)\mathrm{d}x\ \mathrm{d}y\ \mathrm{d}z\right]\mathrm{d}t\,. \qquad [49]$$

The average value of the interfacial area concentration can be obtained by dividing [49] by $V\Omega$. Then, in view of [33], [49] can be rewritten as

$$\overline{\overline{a_i}}^{p3}{}^{t} = \overline{\overline{a_i}}^{t}{}^{p3}, \qquad [50]$$

where operator $\overline{\ }^{p3}$ denotes volume averaging. This shows that the volume average of the time-averaged local interfacial area concentration is identical to the time average of the volume-averaged concentration. This result is similar to that which Delhaye has proved based on the integral method using the Leibnitz rule (Delhaye 1976; 1980). Equation [50] might be called the overall ergodic theorem. Although [50] does not require any statistical assumptions on the characteristic of two-phase flow, its validity is limited to finite volume and time domains. However, this theorem shows a very important relationship between the time and spatial averages. The ergodic theorem indicates that these two averages are consistent and they represent fundamentally similar physical quantities. It is shown below that by introducing some additional conditions, one can obtain the ergodic theorem which is valid locally.

The integration of $a_i(x,y,z,t)$ in the domain of z from z to $z + L$ and t from t to $t + \Omega$ is defined by

$$I(L,\Omega) = \int\int_{L,\Omega} a_i(x,y,z,t)\mathrm{d}z\ \mathrm{d}t\,. \qquad [51]$$

This integral has an important physical meaning because it represents the area of interface in the domain from z to $z + L$ and from t to $t + \Omega$. Now by changing the sequence of integrations,

$$\int_z^{z+L} \left[\int_t^{t+\Omega} a_i(x,y,z,t)\mathrm{d}t\right]\mathrm{d}z = \int_t^{t+\Omega} \left[\int_z^{z+L} a_i(x,y,z,t)\mathrm{d}z\right]\mathrm{d}t\,. \qquad [52]$$

Thus, by dividing [52] by $L\Omega$ one obtains

$$\frac{1}{L}\int_z^{z+L} \left[\frac{1}{\Omega}\int_t^{t+\Omega} a_i(x,y,z,t)\mathrm{d}t\right]\mathrm{d}z = \frac{1}{\Omega}\int_t^{t+\Omega} \left[\frac{1}{L}\int_z^{z+L} a_i(x,y,z,t)\mathrm{d}z\right]\mathrm{d}t\,. \qquad [53]$$

The above equation is a special case of the general ergodic theorem for the interfacial area concentration given by [50]. An ergodic theorem applicable to the local interfacial area concentration can be obtained by considering stationary and developed two-phase flow. For this type of two-phase flow, appropriately averaged two-phase flow parameters are independent of time and axial location. By applying these characteristics to the interfacial area concentration, the following results can be obtained:

$$\bar{a}_i^t \equiv \frac{1}{\Omega}\int_t^{t+\Omega} a_i(x,y,z,t)\mathrm{d}t = A(x,y) \qquad [54]$$

and

$$\bar{a}_i^{pz} \equiv \frac{1}{L}\int_z^{z+L} a_i(x,y,z,t)\mathrm{d}z = B(x,y)\,, \qquad [55]$$

where z is the direction of flow. By substituting [54] and [55] into [53] and integrating it, it can be shown that

$$\frac{1}{L}\int_z^{z+L} A(x,y)\mathrm{d}z = \frac{1}{\Omega}\int_t^{t+\Omega} B(x,y)\mathrm{d}t\,. \qquad [56]$$

This can be satisfied for arbitrary values of x and y only if

$$A(x,y) = B(x,y)\,. \qquad [57]$$

Therefore, for stationary and developed two-phase flow, the linear averaging $\bar{a}_i^{pz}$ and the time averaging $\bar{a}_i^t$ become identical when the linear averaging is taken along the flow direction. Thus,

$$\bar{a}_i^{pz} = \bar{a}_i^t \quad \text{(for stationary and developed flow)}\,. \qquad [58]$$

In comparison with the general ergodic theorem given by [50], [58] can be called the local ergodic theorem. From [29] and [41] this ergodic theorem can be modified to

$$\frac{1}{l}\overline{\frac{1}{\cos\theta}} = \frac{1}{\tau}\overline{\frac{1}{|\mathbf{v}_i|\cos\phi}} \qquad [59]$$

The local ergodic theorem given by [58] is quite important in terms of practical applications. This is because the theorem indicates that the line-averaged interfacial area concentration can be obtained from the time-averaged local interfacial area concentration. The latter can be related to measurable quantities in a two-phase flow system. For example, the time-averaged local interfacial area concentration can be measured from the number of bubbles or drops and the interfacial velocity as shown in [44].

3 METHOD OF MEASUREMENT OF LOCAL INTERFACIAL AREA CONCENTRATION

As discussed in the preceding sections, there are two possible methods for measuring the local interfacial area concentration. The first approach is to use the principle indicated by [32]. Equations [30] and [31] show that one has to measure the number of bubbles or droplets and a direction cosine of a normal vector of each interface in the sufficiently large z axis distance between z and $z + L$. For this, it is necessary to use a sensor which scans distance L in a negligible time duration. In other words, the sensor velocity must be much larger than the velocity of interfaces. An optical technique such as a photographic method may be applied for this purpose. An attempt has been made based on this method (Veteau 1981). However, at present, this approach has a limited success only for very low void

fraction two-phase flow. At higher void fraction, the light scattering and refraction at multiple interfaces become a very serious problem. Due to these difficulties in the experimental technique, a complete measurement of the local interfacial area concentration based on [30]–[32] has not been accomplished yet. In relation to the optical technique, there is a light attenuation method which is based on a different measuring principle. Several attempts have been made using this method (Veteau & Charlot 1981; Trice & Rodger 1956; Ohba 1978).

Another approach is to use a principle indicated by [44]. In view of [42] and [43], this method requires a sensor located in a fixed point in two-phase flow and being capable of measuring the number of bubbles or droplets, their interfacial velocity and the angle between the interfacial velocity and normal vector of the interface. For this purpose, an electrical resistivity probe, optical probe, and anemometer which are often used in two-phase flow measurements (Hewitt 1976; Banerjee & Lahey 1981) may be suitable. In what follows, the measurement using an electrical resistivity probe will be discussed in detail.

Figure 4 schematically shows a double-sensored electrical resistivity probe. Sensors 1 and 2 detect gas and liquid phase by means of the difference between gas and liquid electrical resistivity. Therefore, from the electrical signals out of these sensors, a gas–liquid interface can be detected. Therefore, using these sensors, the number of interfaces passing the probe per unit time N_t can be measured. Furthermore, by measuring the time difference for an interface to pass sensors 1 and 2, the velocity of interface passing the probe can be measured.

Now consider a unit vector $\mathbf{n}_s$ with direction the same as that of a double-sensored probe (figure 4). Its direction cosines are represented by $(\cos \eta_x, \cos \eta_y, \cos \eta_z)$. The position of sensor 1 is given by (x_0,y_0,z_0); then the position of sensor 2 is given by $(x_0 + \Delta s \cos \eta_x, y_0 + \Delta s \cos \eta_y, z_0 + \Delta s \cos \eta_z)$. By considering the jth interface passing the sensors 1 and 2, with the passing velocity of v_{sj} and the time interval of Δt_j, the following relation exists:

$$v_{sj} = \frac{\Delta s}{\Delta t_j}. \qquad [60]$$

Since the jth surface is represented by [19], the surface equation should satisfy

$$f_j(x_0,y_0,z_0,t_j) = 0, \qquad [61]$$

$$f_j(x_0 + \Delta s \cos \eta_x, y_0 + \Delta s \cos \eta_y, z_0 + \Delta s \cos \eta_z, t_j + \Delta t_j) = 0, \qquad [62]$$

where t_j is the time when the jth interface passes the sensor 1. When Δs is small, [61] and [62] give the approximate relation

$$\frac{\partial f_j}{\partial x} \cos \eta_x + \frac{\partial f_j}{\partial y} \cos \eta_y + \frac{\partial f_j}{\partial z} \cos \eta_z = -\frac{\partial f_j}{\partial t} / v_{sj}. \qquad [63]$$

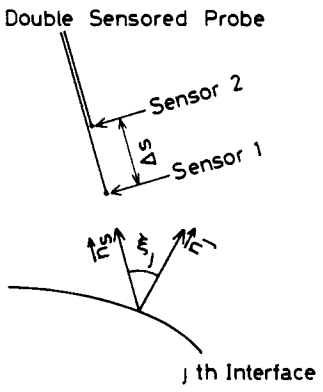

Figure 4. Double-sensored probe and jth interface

Equation [63] indicates that it is possible to calculate the value given by [36] by using three double-sensored probes with a common sensor. It is schematically shown in figure 5. The unit vector and its direction cosines for probe k are represented by $\mathbf{n}_{sk}$ and ($\cos\ \eta_{xk}$, $\cos\ \eta_{yk}$, $\cos\ \eta_{zk}$) with $k = 1, 2, 3$. The passing velocity of the jth interface over probe k is denoted by v_{skj}.

The directions of three probes can be made independent, which implies that the determinant $|A_0|$ should satisfy

$$|A_0| \equiv \begin{vmatrix} \cos\ \eta_{x1}, \cos\ \eta_{y1}, \cos\ \eta_{z1} \\ \cos\ \eta_{x2}, \cos\ \eta_{y2}, \cos\ \eta_{z2} \\ \cos\ \eta_{x3}, \cos\ \eta_{y3}, \cos\ \eta_{z3} \end{vmatrix} \neq 0 . \qquad [64]$$

Under this condition [63] has a solution. From this solution it can be shown that

$$(|\mathbf{v}_{ij}|\cos\ \phi_j)^{-1} = \frac{\sqrt{|A_1|^2 + |A_2|^2 + |A_3|^2}}{\sqrt{|A_0|^2}} , \qquad [65]$$

where $|A_1|$, $|A_2|$, and $|A_3|$ are given by

$$|A_1| \equiv \frac{1}{v_{s1j}} \begin{vmatrix} 1, \cos\ \eta_{y1}, \cos\ \eta_{z1} \\ 1, \cos\ \eta_{y2}, \cos\ \eta_{z2} \\ 1, \cos\ \eta_{y3}, \cos\ \eta_{z3} \end{vmatrix} , \qquad [66]$$

$$|A_2| \equiv \frac{1}{v_{s2j}} \begin{vmatrix} \cos\ \eta_{x1}, 1, \cos\ \eta_{z1} \\ \cos\ \eta_{x2}, 1, \cos\ \eta_{z2} \\ \cos\ \eta_{x3}, 1, \cos\ \eta_{z3} \end{vmatrix} , \qquad [67]$$

$$|A_3| \equiv \frac{1}{v_{s3j}} \begin{vmatrix} \cos\ \eta_{x1}, \cos\ \eta_{y1}, 1 \\ \cos\ \eta_{x2}, \cos\ \eta_{y2}, 1 \\ \cos\ \eta_{x3}, \cos\ \eta_{y3}, 1 \end{vmatrix} . \qquad [68]$$

If three orthogonal probes are used, for example, by chosing x, y, and z as the directions of the three double-sensored probes, then the result can be simplified to

$$\bar{a}_i^j = \frac{1}{\Omega} \sum_j \left\{ \left(\frac{1}{v_{s1j}}\right)^2 + \left(\frac{1}{v_{s2j}}\right)^2 + \left(\frac{1}{v_{s3j}}\right)^2 \right\}^{1/2} . \qquad [69]$$

Thus the local time-averaged interfacial area can be measured by three interfacial velocity components. Although in principle this method gives accurate measurements of an interfacial

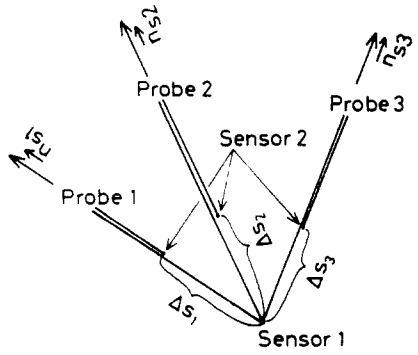

Figure 5 Three double-sensored probes

area concentration, there are some problems in terms of practical applications. In deriving [65] from [61] and [62], it has been assumed that Δs is small. In view of the effect of curvature of bubble or droplet interfaces, the accuracy of the measurement increases as Δs decreases. On the other hand, [60] indicates that Δt_j decreases with decreasing Δs. This implies that one has to measure smaller Δt_j as Δs decreases. Then the accuracy of measuring Δt_j and that of v_{ij} decreases as Δs becomes smaller. Therefore, in practical measurements, the determination of optimum Δs should be an important problem which requires utmost attention.

The above described method based on the three double-sensored probes may be difficult to apply if the required sensor distance is very small. It is evident that Δs should be considerably smaller than a bubble or drop diameter. Furthermore, deformations of interfaces by the probes should also be carefully examined. It can be said that this method will encounter increasing difficulties as the fluid particle size becomes smaller. In view of the above, a simpler probe method which can be applied to many two-phase conditions is highly desirable. One possiblity is to use a single double-sensored probe. However, in this case it becomes necessary to assume certain statistical characteristics of two-phase flow.

Now a double-sensored probe located in the z direction is considered where the mean flow is assumed to also be in the z direction. The velocity and the normal unit vector of the jth interface, $\mathbf{v}_{ij}$ and $\mathbf{n}_j$, can be given in terms of unit vectors $\mathbf{n}_x$, $\mathbf{n}_y$, and $\mathbf{n}_z$, using angles with z and y axes given by (α_j,β_j) and (μ_j,ν_j) and shown in figures 6 and 7. Thus,

$$\begin{aligned} \mathbf{v}_{ij} &= |\mathbf{v}_{ij}|\{\cos\ \alpha_j\ \mathbf{n}_z + \sin\ \alpha_j\ \cos\ \beta_j\ \mathbf{n}_y + \sin\ \alpha_j\ \sin\ \beta_j\ \mathbf{n}_x\}\ , \\ \mathbf{n}_j &= \cos\ \mu_j\ \mathbf{n}_z + \sin\ \mu_j\ \cos\ \nu_j\ \mathbf{n}_y + \sin\ \mu_j\ \sin\ \nu_j\ \mathbf{n}_x\ . \end{aligned} \qquad [70]$$

By assuming that there are no statistical correlations between $|\mathbf{v}_{ij}|$ and ϕ_j (randomness of $\mathbf{v}_{ij}$), and in view of [70],

$$\begin{aligned} \overline{\frac{1}{|\mathbf{v}_i|\cos\ \phi}} &= \left\{\sum_j \frac{1}{|\mathbf{v}_{ij}|}\Big/\left(\sum_j\right)\right\} \\ &\times \left[\sum_j \frac{1}{\{\cos\ \alpha_j\ \cos\ \mu_j + \sin\ \alpha_j\ \sin\ \mu_j\ \cos\ (\beta_j - \nu_j)\}}\right]\Big/\left(\sum_j\right). \end{aligned} \qquad [71]$$

When the number of measured interfaces is large, the summation can be approximated by an integration. Thus,

$$\overline{\frac{1}{|\mathbf{v}_i|\cos\ \phi}} = \left\{\sum_j \frac{1}{|\mathbf{v}_{ij}|}\Big/\left(\sum_j\right)\right\} \cdot \int\int\int\int \frac{P(\alpha,\beta,\mu,\nu)\mathrm{d}\alpha\ \mathrm{d}\beta\ \mathrm{d}\mu\ \mathrm{d}\nu}{\{\cos\ \alpha\ \cos\ \mu + \sin\ \alpha\ \sin\ \mu\ \cos\ (\beta-\nu)\}}\ , \qquad [72]$$

where $P(\alpha,\beta,\mu,\nu)$ is a probability density function of α, β, μ, ν.

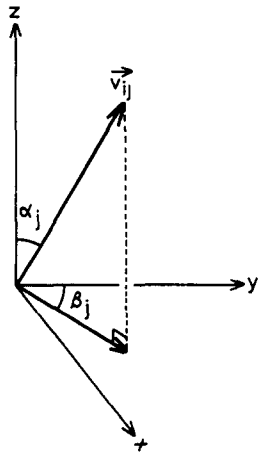

Figure 6. Angles α_j and β_j for $\mathbf{v}_{ij}$.

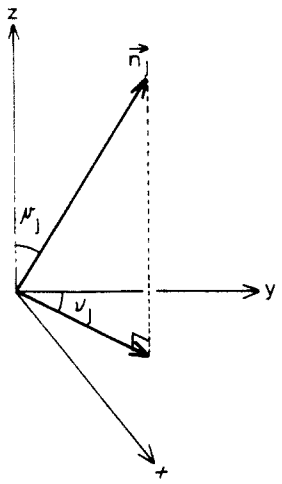

Figure 7. Angles μ_j and ν_j for $\mathbf{n}_j$

On the other hand, in view of [61] and [62], the measured velocity v_{sz} associated with the jth interface passing the double-sensored probe located in the z direction is given by

$$|v_{szj}|\cos\ \mu_j = |\mathbf{v}_{ij}|\cos\ \phi_j\,. \qquad [73]$$

In view of [73], and assuming that no statistical correlation exists between $|\mathbf{v}_{ij}|$ and μ_j, it can be shown that

$$\sum_j \frac{1}{|v_{szj}|}\Big/\left(\sum_j\right) = \left\{\sum_j \frac{1}{|\mathbf{v}_{ij}|}\Big/\left(\sum_j\right)\right\}\int\int\int\int \frac{P(\alpha,\beta,\mu,\nu)\cos\ \mu\ \mathrm{d}\alpha\ \mathrm{d}\beta\ \mathrm{d}\mu\ \mathrm{d}\nu}{\{\cos\ \alpha\ \cos\ \mu + \sin\ \alpha\ \sin\ \mu\ \cos\ (\beta-\nu)\}}\,, \qquad [74]$$

where $0 \leqq \alpha,\ \mu \leqq \pi/2$ and $0 \leqq \beta,\ \nu \leqq 2\pi$.

In view of [72], [74], and [41], the time-averaged local interfacial area concentration is given in terms of the measured velocities of interfaces and the probability density function. Hence

$$\bar{a}_i^t\,(x_0,y_0,z_0) = \frac{1}{\tau}\left\{\sum_j \frac{1}{|v_{szj}|}\Big/\left(\sum_j\right)\right\} \times \frac{\int\int\int\int \dfrac{P(\alpha,\beta,\mu,\nu)\ \mathrm{d}\alpha\ \mathrm{d}\beta\ \mathrm{d}\mu\ \mathrm{d}\nu}{\{\cos\ \alpha\ \cos\ \mu + \sin\ \alpha\ \sin\ \mu\ \cos\ (\beta-\nu)\}}}{\int\int\int\int \dfrac{P(\alpha,\beta,\mu,\nu)\cos\ \mu\ \mathrm{d}\alpha\ \mathrm{d}\beta\ \mathrm{d}\mu\ \mathrm{d}\nu}{\{\cos\ \alpha\ \cos\ \mu + \sin\ \alpha\ \sin\ \mu\ \cos\ (\beta-\nu)\}}} \qquad [75]$$

Equation [75] indicates that $\bar{a}_i^t$ can be calculated from measured values of the bubble or droplet number N_t and of the passing velocities of interfaces using one double-sensored probe. However, in addition to these it is necessary to assume a form of the probability density function $P(\alpha,\beta,\mu,\nu)$. For this purpose, it is assumed that the interfaces are composed of spherical bubbles or droplets and the probe passes every part of bubble or droplet with an equal probability. Furthermore, it is assumed that the x and y direction components of $\mathbf{v}_{ij}$ are random. Under these assumptions, β and ν takes any value between 0 and 2 π with equal probability and β and ν are statistically independent of each other. Then the probability density function can be reduced to

$$P(\alpha,\beta,\mu,\nu)\mathrm{d}\alpha\ \mathrm{d}\beta\ \mathrm{d}\mu\ \mathrm{d}\nu = P(\alpha,\mu,(\beta-\nu))\mathrm{d}\alpha\ \mathrm{d}\mu\ \mathrm{d}(\beta-\nu)$$

$$= \frac{1}{\pi}g(\alpha)\sin\ \mu\ \cos\ \mu\ \mathrm{d}\alpha\ \mathrm{d}\mu\ \mathrm{d}(\beta-\nu)\,. \qquad [76]$$

where $g(\alpha)$ is a probability density function of angle α. By substituting [76] into [75] and in view of [43], one finally obtains the following result after carrying out the integration:

$$\bar{a}_i'(x_0,y_0,z_0) = 4N_t \left\{ \sum_j \frac{1}{|v_{szj}|} \Big/ \left(\sum_j \right) \right\} \frac{1}{1 + \int_0^{\pi/2} g(\alpha) \sin \alpha \ln ((1 + \cos \alpha)/\sin \alpha)\, d\alpha} \Big/ \int_0^{\pi/2} g(\alpha) \cos \alpha \, d\alpha \quad [77]$$

Since the main flow is in the z direction, the major component of the interfacial velocity is also the z component if the mean flow velocity is not small compared with the fluctuating x and y components. In that case, $g(\alpha)$ is considered to have a sharp peak at $\alpha = 0$. Hence as a first approximation, $g(\alpha)$ may be represented by a delta function as

$$g(\alpha) = \delta(\alpha) . \quad [78]$$

Then [77] can be simplified to

$$\bar{a}_i'(x_0,y_0,z_0) = 4N_t \left\{ \sum_j \frac{1}{|v_{szj}|} \Big/ \left(\sum_j \right) \right\} = 4N_t \frac{\overline{1}}{|v_{sz}|} . \quad [79]$$

The approximation given by [78] implies that the interfacial velocity $\mathbf{v}_{ij}$ has only the z component. Equation [79] has also been obtained by Sekoguchi *et al.* (1974a; 1974b), Sekoguchi (1982), Herringe *et al.* (1976), Veteau (1981), and Veteau & Charlot (1981) based on the bubble diameter distribution assuming spherical bubble.

A more accurate approximation for $g(\alpha)$ may be given by

$$\begin{aligned} g(\alpha) &= \frac{1}{\alpha_0} \quad \text{for } 0 < \alpha < \alpha_0 , \\ &= 0 \quad \text{for } \alpha_0 < \alpha < \frac{\pi}{2} . \end{aligned} \quad [80]$$

This form of $g(\alpha)$ implies that the angle α made by the interfacial velocity and the z axis is random with an equal probability within the maximum angle of α_0. Substituting [80] into [77], the interfacial area concentration becomes

$$\bar{a}_i'(x_0,y_0,z_0) = \frac{4N_t \left\{ \sum_j \frac{1}{|v_{szj}|} \Big/ \left(\sum_j \right) \right\}}{1 - \cot\frac{1}{2}\alpha_0 \ln\left(\cos\frac{1}{2}\alpha_0\right) - \tan\frac{1}{2}\alpha_0 \ln\left(\sin\frac{1}{2}\alpha_0\right)} . \quad [81]$$

Therefore, by knowing the value of α_0, the time-averaged local interfacial area concentration can be calculated from the measured values of N_t and v_{szj}. α_0 can be estimated from measured values of statistical parameters of interfacial velocity as explained elsewhere (Kataoka *et al.* 1984) (see also the Appendix). It is given by

$$\frac{\sin 2\alpha_0}{2\alpha_0} = \frac{1 - (\sigma_z^2/\overline{|\mathbf{v}_{sz}|^2})}{1 + 3(\sigma_z^2/\overline{|\mathbf{v}_{sz}|^2})} . \quad [82]$$

Thus by knowing the mean value and fluctuations of the z component interfacial velocity, which are denoted by $\overline{|\mathbf{v}_{sz}|}$ and σ_z, it is possible to estimate the value of α_0.

4. EXPERIMENTAL VALUE OF LOCAL INTERFACIAL AREA CONCENTRATION

As shown in the previous section, the time-averaged local interfacial area concentration can be calculated from measured values of the bubble or droplet number per unit time and mean and fluctuating components of the interfacial velocity using [81] and [82].

Serizawa *et al.* (1974; 1975a; 1975b; 1975c) have measured the above mentioned parameters in air–water bubbly and slug flow in a vertical tube of inner diameter of 6 cm Under stationary and developed conditions, they measured the bubble number per unit time N_t and spectrum of passing velocity of interface $|v_{gz}|$ at various radial positions. The examples of the spectra of $|v_{gz}|$ are shown in figure 8. From these spectra, one can calculate the reciprocal of a harmonic mean of $|v_{gz}|$ as

$$\overline{\frac{1}{|v_{gz}|}} = \left\{ \sum_j \frac{1}{|v_{gzj}|} \Big/ \left(\sum_j \right) \right\} = \int_0^\infty \frac{w(|v_{gz}|)}{|v_{gz}|} \, \mathrm{d}|v_{gz}| , \qquad [83]$$

where $w(|v_{gz}|)$ is the probability density function of $|v_{gz}|$ corresponding to the normalized spectrum shown in figure 8. Similarly, the square mean σ_{gz}^2 of the fluctuation of $|v_{gz}|$ can be calculated from the spectra as

$$\begin{aligned} \sigma_{gz}^2 &= \left\{ \sum_j (|v_{gzj}| - \overline{|v_{gz}|})^2 \Big/ \left(\sum_j \right) \right\} \\ &= \int_0^\infty |v_{gz}|^2 \, w(|v_{gz}|) \, \mathrm{d}|v_{gz}| - \left\{ \int_0^\infty |v_{gz}| \, w(|v_{gz}|) \, \mathrm{d}|v_{gz}| \right\}^2 , \end{aligned} \qquad [84]$$

where

$$\overline{|v_{gz}|} = \int_0^\infty |v_{gz}| \, w(|v_{gz}|) \, \mathrm{d}|v_{gz}| . \qquad [85]$$

The value of $\sigma_z^2/\overline{|\mathbf{v}_{iz}|}^2$ is not measured in Serizawa's experiment. However, one can approximate this value as

$$\frac{\sigma_z^2}{\overline{|\mathbf{v}_{iz}|}^2} \simeq \frac{\sigma_{gz}^2}{\overline{|v_{gz}|}^2} , \qquad [86]$$

which is calculated by [84] and [85] from the measured spectrum of $|v_{gz}|$. Thus, one obtains the local interfacial area concentration from [81] and [82] using the measured values of N_t and spectrum of $|v_{gz}|$. Here α_0 calculated from [82] ranged from 0.17 to 0.39 rad for Serizawa's experiments (Serizawa *et al.* 1974; 1975a; 1975b; 1975c).

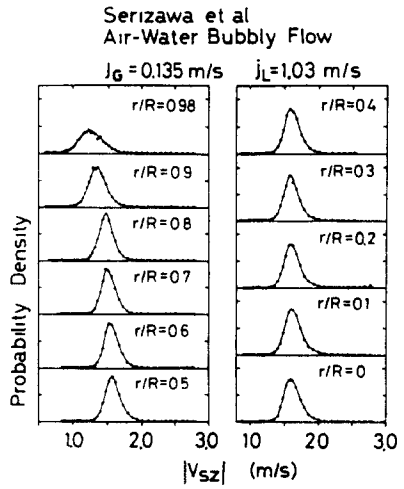

Figure 8 Spectra of $|v_{gz}|$ for air–water bubbly flow at j_G = 0.135 m/s and j_L = 1 03 m/s at various radial positions (Serizawa *et al.*).

Figures 9–15 show some examples of the local interfacial area concentration profiles based on the above-described method and the experimental data of Serizawa *et al.* (1974; 1975a; 1975b; 1975c). In the figures, r denotes a radial position and R denotes radius of flow passage. For bubbly flow the local interfacial area concentration shows rather uniform values in the center region of the tube and higher values near the tube wall. A similar trend of interfacial area concentration has been observed by Veteau (1981) and Veteau & Charlot (1981). The higher values suggest that in this type of bubbly flow the interfacial transport of momentum and heat is higher near the tube wall. On the other hand, in slug flow and bubbly to slug transition flows the local interfacial area concentration does not show an appreciable peak value near the tube wall as indicated in figures 13 and 14. However, higher values of the interfacial area concentration appear at the central region of the tube. It has been already shown by Ishii *et al.* (1982) and Sekoguchi (1982) that the area-averaged interfacial area concentration is strongly dependent on two-phase flow regimes. However, the present study has demonstrated that a transverse profile of the local interfacial area concentration is also strongly dependent on the flow regimes. These results indicate that the interfacial transports of mass, momentum, and energy strongly depend on the overall flow regimes as well as on detailed transverse structures of flow.

Figure 15 shows the radial profiles of various local parameters of two-phase flow along with the interfacial area concentration. This figure suggests that the turbulent velocity of the liquid phase $\tilde{u}_L$ and the void fraction $\bar{\alpha}$ are closely related to the local interfacial area concentration as pointed out by Serizawa (1983) and Herringe *et al.* (1976). The near wall peak of the interfacial area concentration in this particular bubbly flow is matched by the peak of the void fraction. It is noted that the radial profile of the void fraction in bubbly flow strongly depends on inlet conditions (Sekoguchi *et al.* 1974a; 1974b; Sekoguchi 1982). Thus it is considered that the radial profile of the interfacial area concentration depends on inlet conditions.

Here the local interfacial area concentration has been calculated from [81] and [82] using the experimental data obtained from one double-sensored probe. This procedure is based on several assumptions on statistical characteristics of the interface motion as described in the previous section, such as the randomness of the interfacial velocity and equilateral fluctuations of the velocity, etc. These assumptions are considered to be valid in the central region of bubbly flow. The randomness of bubble behavior in this region is experimentally supported by Serizawa *et al.* (1974; 1975a; 1975b; 1975c). However, in the very near the wall region of bubbly flow or slug flow, some of the assumptions are not completely valid.

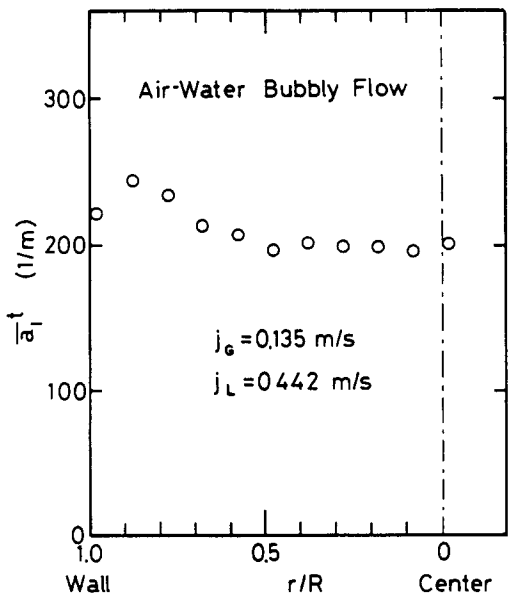

Figure 9. Radial profile of $\bar{a}_i^t$ for air–water bubbly flow at $j_G = 0.135$ m/s and $j_L = 0.442$ m/s calculated from the data of Serizawa *et al.*

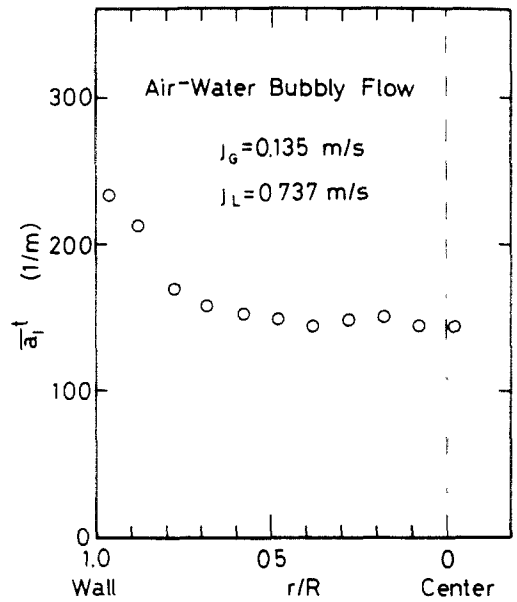

Figure 10 Radial profile of $\bar{a}_i^t$ for air–water bubbly flow at J_G = 0.135 m/s and J_L = 0.737 m/s calculated from the data of Serizawa *et al*

For slug flow, the applicability of the present method depends on the structure of the liquid slug section. If the liquid slugs have only a few bubbles, the interfacial area is mainly determined by the surface area of big slug bubbles. Then the present method may not be accurate. However, if many small bubbles exist in the liquid slugs, these bubbles significantly contribute to the interfacial area concentration. For such a case, the present method may still be applicable. The cases in figures 13 and 14 correspond to the second situation. Furthermore, for two-phase flow where fluid particles cannot be well defined, such as churn-turbulent flow, the above method may not be appropriate. For these circumstances, more information on the interfacial velocity is necessary for an accurate measurement of the local interfacial area concentration. The three double-sensored probe method which is described in the previous section is suitable for this purpose. Such detailed measurements are strongly recommended for a better understanding of two-phase flow structures and interfacial transport phenomena.

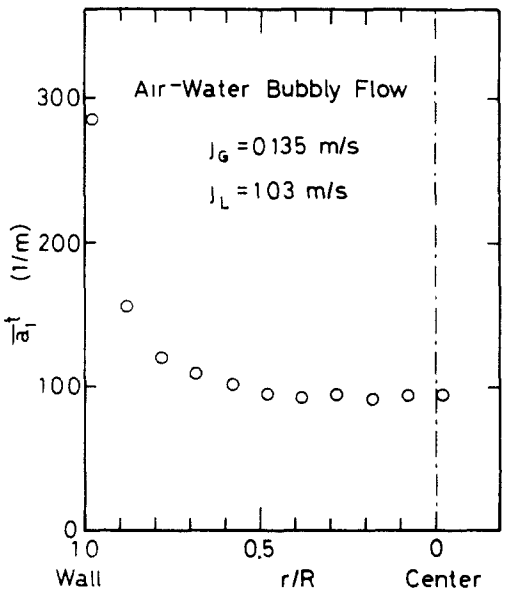

Figure 11 Radial profile of $\bar{a}_i^t$ for air–water bubbly flow at J_G = 0.135 m/s and J_L = 1.03 m/s calculated from the data of Serizawa *et al*

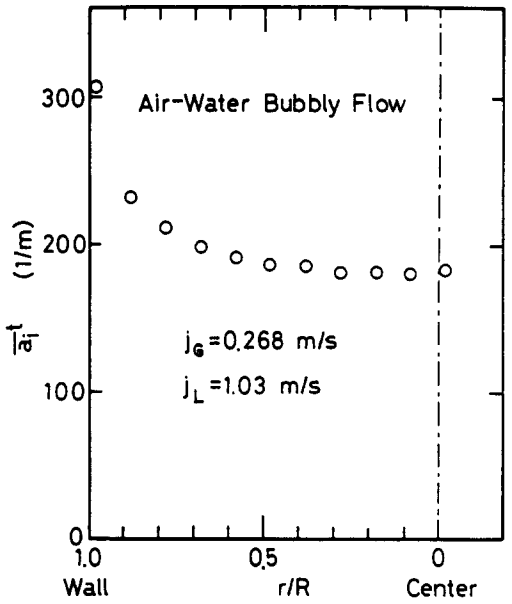

Figure 12. Radial profile of $\bar{a}_i^t$ for air–water bubbly flow at $j_G = 0.268$ m/s and $j_L = 1.03$ m/s calculated from the data of Serizawa *et al.*

5. CONCLUSIONS

The local instantaneous formulation of the interfacial area concentration has been introduced based on the concept of a distribution. Using a delta function and the interface equation, the local instantaneous interfacial area concentration has been defined. Then by integrating the local instantaneous interfacial area concentration, spatial and time-averaged interfacial area concentrations have been obtained. For a dispersed two-phase flow the spatial-(linear-) averaged interfacial area concentration is given in terms of the number of interfaces per unit length and the harmonic mean of cos θ_j, where θ_j is the angle between the normal vector of the jth interface and averaging direction. On the other hand, the time-averaged interfacial area concentration is given in terms of the number of interfaces per unit time and the harmonic mean of $|\mathbf{v}_{ij}| \cos \phi_j$, where $|\mathbf{v}_{ij}|$ is the interfacial velocity of the jth surface and ϕ_j is the angle between $\mathbf{v}_{ij}$ and the normal vector of jth interface.

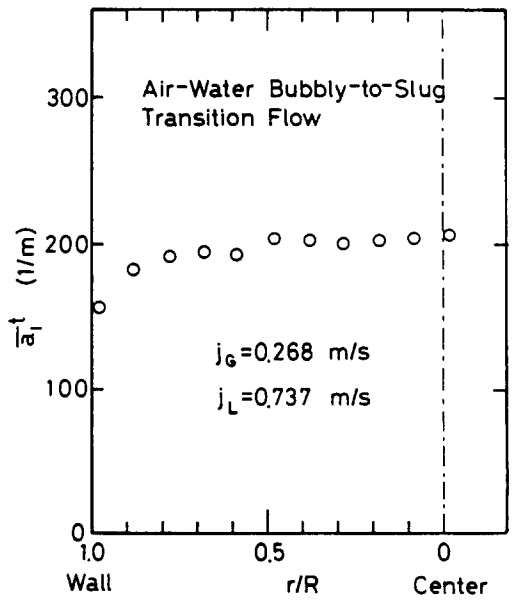

Figure 13 Radial profile of $\bar{a}_i^t$ for air–water bubble-to-slug-transition flow at $j_G = 0.268$ m/s and $j_L = 0.737$ m/s calculated from the data of Serizawa *et al*

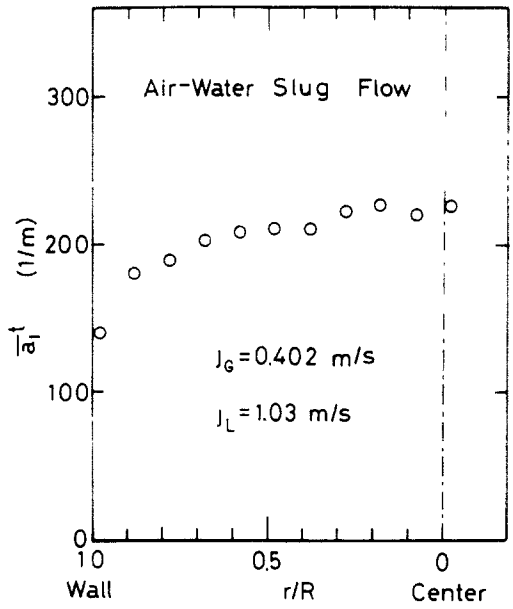

Figure 14 Radial profile of $\bar{a}_i^t$ for air–water slug flow at $j_G = 0.402$ m/s and $j_L = 1.03$ m/s calculated from the data of Serizawa *et al.*

Based on the local instantaneous formulation of the interfacial area concentration, several ergodic theorems concerning the averaged interfacial area concentration have been derived. The overall ergodic theorem for the time and spatial averages has been obtained theoretically. For a stationary and developed two-phase flow, the local ergodic theorem is obtained. Both theorems are important in terms of practical applications and interpretations of experimental data.

Based on these theoretical developments, several measurement methods for the interfacial area concentration have been proposed and discussed in detail. The method using three double-sensored probes located in three independent directions has been proposed for a general application. It is shown that this method enables an accurate measurement of the local interfacial area concentration. However, it is also pointed out that the required small size of the whole probe may be an engineering problem.

A much simpler method using one double-sensored probe is also proposed and discussed in detail. By assuming certain statistical characteristics of the interfacial motion, an expression for the local interfacial area concentration can be related to measurable quantities from a double-sensored probe.

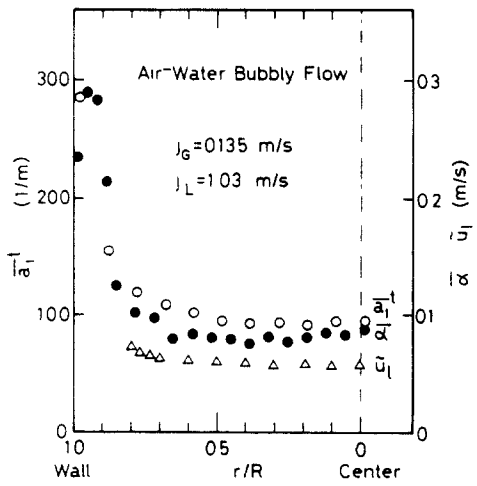

Figure 15 Radial profiles of $\bar{a}_i^t$, $\bar{\alpha}$ (void fraction), and $\bar{u}_L$ (turbulent velocity of liquid) at $j_G = 0.135$ m/s and $j_L = 1.03$ m/s (Serizawa *et al.*)

Applying this one-probe method to experimental data, radial profiles of the local interfacial area concentration have been obtained for air–water bubbly and slug flow. The local interfacial area concentration has a peak value near the tube wall in the bubbly flow, while in slug flow it has higher values in the central region of two-phase flow. These results demonstrated the applicability of the one double-sensored probe method for the measurement of the local interfacial area concentration.

The formulation of the local interfacial area concentration and measuring methods developed in this study are basically applicable to any type of two-phase flow. A further experimental study utilizing these methods for measuring the interfacial area concentration is highly desirable. Such a detailed measurement of the local quantities of two-phase flow greatly increases the understanding of interfacial transport phenomena, structures of two-phase flow, and flow regimes.

Acknowledgments —The authors would like to express their appreciation to Dr. N. Zuber and Mr. M. Young of NRC for valuable discussions on the subject. A part of this work was performed under the auspices of the U. S. Nuclear Regulatory Commission.

NOMENCLATURE

a_i	interfacial area concentration
$a_i(x)$	local interfacial area concentration (one dimensional)
$a_i(x,y,z,t)$	local instantaneous interfacial area concentration
$\bar{a}_i^p$	spatial averaging of $a_i(x,y,z,t)$
$\bar{a}_i^{p3}$	volume averaging of $a_i(x,y,z,t)$
$\bar{a}_i^{pz}$	linear (z direction) averaging of $a_i(x,y,z,t)$
$\bar{a}_i^t$	time averaging of $a_i(x,y,z,t)$
$A(x,y)$	function of x and y
$A_0 \sim A_3$	determinant given by [64] and [66]–[68]
$B(x,y)$	function of x and y
$\overline{(1/\cos\ \theta)}$	reciprocal of harmonic mean of cos θ_j [30]
$\cos\ \eta_x$,	direction cosines of $\mathbf{n}_s$
$\cos\ \eta_y$,	
$\cos\ \eta_z$	
$\cos\ \eta_{xk}$,	direction cosines of $\mathbf{n}_{sk}$
$\cos\ \eta_{yk}$,	
$\cos\ \eta_{zk}$	
$f(x,y,z,t)$	function representing an interface
$f_j(x,y,z,t)$	function representing jth interface
$\mathbf{g}$	acceleration due to gravity
$g(\alpha)$	probability density function of α
grad f,	gradient of $f(x,y,z,t)$
grad f_j	gradient of $f_j(x,y,z,t)$
h_{ki}	heat transfer coefficient at interface
H_k	enthalpy of k phase
$I(V,\Omega)$	integration of $a_i(x,y,z,t)$ in domain V and Ω
$I(L,\Omega)$	integration of $a_i(x,y,z,t)$ in domain L and Ω
j_G, j_L	superficial velocity for gas and liquid
l	length scale given by [31], reciprocal of number of interfaces per unit length
L	length in z direction
L_s	length scale at interface given by [4]
m_k	mean mass transfer per unit area for k phase
M_{ik}	interfacial force for k phase
n	number
$\mathbf{n}_j$	unit normal vector of jth interface

$\mathbf{n}_s$	unit vector in the direction of probe
$\mathbf{n}_{sk}$	unit vector in the direction of kth probe
$\mathbf{n}_x$, $\mathbf{n}_y$, $\mathbf{n}_z$	unit vector in x, y, z directions
N_t	number of bubbles or droplets passing a point per unit time
N_z	number of bubbles or droplets per unit length
p_k	pressure of k phase
$P(\alpha,\beta,\mu,\nu)$	probability density function of α, β, μ, ν
$P(\alpha,\mu,(\beta-\nu))$	probability density function of α, μ, $(\beta-\nu)$
$\bar{q}_k$	mean conduction heat flux of k phase
q'_k	turbulent heat flux of k phase
q''_k	interfacial heat flux
r	radial position
R	radius of flow passage
t	time when average is taken
t_0	fixed time
t_j	time given by [34]
T	temperature at interface
T_k	bulk temperature of k phase
$\tilde{u}_l$	turbulence velocity of liquid phase
$\mathbf{v}_{ij}$	velocity of jth interface
$\overline{\lvert\mathbf{v}_i\rvert}$, $\overline{\lvert\mathbf{v}_i\rvert^2}$	arithmetic means of $\lvert\mathbf{v}_{ij}\rvert$ and $\lvert\mathbf{v}_{ij}\rvert^2$
$\overline{1/\lvert\mathbf{v}_i\rvert}$	reciprocal of harmonic mean of $\lvert\mathbf{v}_{ij}\rvert$
$\overline{1/\lvert\mathbf{v}_i\rvert\cos\phi}$	reciprocal of harmonic mean of $\lvert\mathbf{v}_{ij}\rvert\cos\phi_j$
$\mathbf{v}_{ixj}$, $\mathbf{v}_{iyj}$, $\mathbf{v}_{izj}$	x, y, and z components of $\mathbf{v}_{ij}$
$\overline{\mathbf{v}_{ix}}$, $\overline{\mathbf{v}_{iy}}$, $\overline{\mathbf{v}_{iz}}$	arithmetic mean of $\mathbf{v}_{ixj}$, $\mathbf{v}_{iyj}$, and $\mathbf{v}_{izj}$
$\overline{\lvert\mathbf{v}_{ix}\rvert^2}$, $\overline{\lvert\mathbf{v}_{iy}\rvert^2}$, $\overline{\lvert\mathbf{v}_{iz}\rvert^2}$	arithmetic mean of $\lvert\mathbf{v}_{ixj}\rvert^2$, $\lvert\mathbf{v}_{iyj}\rvert^2$, and $\lvert\mathbf{v}_{izj}\rvert^2$
$\mathbf{v}_k$	velocity of k phase
v_{sj}	passing velocity of jth interface through double-sensored probe
v_{skj}	passing velocity of jth interface through kth double-sensored probe
v_{szj}	passing velocity of jth interface through double-sensored probe in z direction
$\overline{1/\lvert v_{sz}\rvert}$	reciprocal of harmonic mean of $\lvert v_{szj}\rvert$
$\overline{\lvert v_{sz}\rvert}$	arithmetic mean of $\lvert v_{szj}\rvert$
V	volume
$w(\lvert v_{sz}\rvert)$	probability density function of $\lvert v_{sz}\rvert$
x, y, z	coordinates
x_0,y_0,z_0	fixed point in x, y, and z coordinate
z_j	z coordinate given by [22]
z	axial coordinate

Greek symbols

$\bar{\alpha}$	void fraction
α_k	volume fraction of k phase
α_j	angle between $\mathbf{v}_{ij}$ and $\mathbf{n}_z$
α_0	angle given by [80]
β_j	angle between $\mathbf{n}_y$ and projection of $\mathbf{v}_{ij}$ into x–y plane
γ	constant
Γ_k	mass generation of k phase
$\delta(x)$	delta function
Δt_j, Δt_{jk}	time lag of (jth) interface passing between sensor 1 and 2 of (kth) double sensored probe
Δx	spacing in x direction
Δs	distance between sensor 1 and 2 of double-sensored probe
θ_j	angle between $\mathbf{n}_z$ and $\mathbf{n}_j$
μ_j	angle between $\mathbf{n}_z$ and $\mathbf{n}_j$

ν_j	angle between $\mathbf{n}_y$ and projection of $\mathbf{v}_{ij}$ into $x-y$ plane
ξ_j	angle between $\mathbf{n}_s$ and $\mathbf{n}_j$
ρ_k	density of k phase
σ_x, σ_y, σ_z, σ_{sz}	root mean square of fluctuating components of $\mathbf{v}_{ixj}$, $\mathbf{v}_{iyj}$, $\mathbf{v}_{izj}$, and $\lvert v_{szj}\rvert$
τ	time scale given by [39], reciprocal of number of interfaces passing a point per unit time
τ_i	average interfacial shear stress
$\bar{\bar{\tau}}_k$	average viscous stress for k phase
τ'_k	turbulent shear stress for k phase
ϕ_j	angle between $\mathbf{n}_j$ and $\mathbf{v}_{ij}$
$\phi(x)$	arbitrary function
Φ_k	energy dissipation for k phase
Ω	time duration

Subscripts

L	liquid phase
G	gas phase
i	value at interface
k	k phase (gas or liquid)

REFERENCES

BANERJEE, S. & LAHEY, R. T., JR., 1981 *Advances in Two-Phase Flow Instrumentation, Advances in Nuclear Science Technology* (Edited by J. Lewin and M. Becker), Vol. 13, pp. 227–414. Plenum Press, New York.

DELHAYE, J. M. 1968 Equations fondamentales des écoulements diphasiques, Parts 1 and 2. CEA-R-3429, Centre d'Etudes Nucléaires de Grenoble, France.

DELHAYE, J. M. 1976 Sur les surfaces volumiques locale et intégrale en ecoulement diphasiques. *C. R. Acad. Sci. Paris Série A* **282**, 243–246.

DELHAYE J. M., GIOT, M. & RIETHMULLER, M. L. 1980 *Thermohydraulics of Two-Phase Systems for Industrial Design and Nuclear Engineering,* Chap. 9. Hemisphere, New York.

DIRAC, P. A. M. 1958 *The Principles of Quantum Mechanics*, 4th Edn. OUP, Oxford.

HERRINGE R. A. & DAVIS, M. R. 1976 Structural development of gas–liquid mixture flows. *J. Fluid Mech.* **73**, 97–123.

HEWITT, G. F. & LOVEGROVE, P. C. 1976 Experimental Methods in Two-Phase Flow Studies, EPRI NP-118, Electrical Power Research Inst.

ISHII, M. 1975 *Thermo-fluid Dynamic Theory of Two-phase Flow.* Eyrolles, Paris/Scientific and Medical Publications of France, New York.

ISHII, M. 1977 One-Dimensional Drift-Flux Model and Constitutive Equations for Relative Motion between Phases in Various Flow Regimes, ANL-77-47, Argonne National Laboratory, Argonne, Ill.

ISHII, M. & MISHIMA, K. 1980 Study of two-fluid model and interfacial area, ANL-80-111, NUREG/CR-1873, Argonne National Laboratory, Argonne, Ill.

ISHII, M., MISHIMA, K., KATAOKA, I. & KOCAMUSTAFAOGULLARI, G. 1982 Two-phase fluid model and importance of the interfacial area in two-phase flow analysis, *Proc. 9th U. S. National Congress of Applied Mechanics*, pp 73-80, Ithaca, New York, June 21–25.

KATAOKA, I., ISHII, M. & SERIZAWA, A. 1984 Local Formulation of Interfacial Area Concentration and Its Measurements in Two-phase Flow, ANL-84-68, NUREG/CR-4029, Argonne National Laboratory, Argonne, Ill.

KOCAMUSTAFAOGULLARI, G. & ISHII, M. 1983 Interfacial area and nucleation site density in boiling systems. *Int. J. Heat Mass Trans.* **26**, 1377–1387.

OHBA, K. 1978 Measurement of interfacial area and void fraction in bubbly flow, *15th National Heat Transfer Sym.* Japan, pp 331–333.

SCHWARTZ, L. 1950–1951 *Théorie des Distributions I, II,* Editions Scientifiques. Hermann, Paris.

SCHWARTZ, L. 1961 *Méthodes Mathématiques pour les Sciences Physiques*, Editions Scientifiques. Hermann, Paris

SEKOGUCHI, K., FUKUI, H., MATSUOKA, T. & NISHIKAWA, K. 1974a Studies on statistical characteristics of bubbles by electrical resistivity probe I *Trans. JSME* **40**(336), 2295–2301.

SEKOGUCHI, K., FUKUI, H., TUTUI, M. & NISHIKAWA, K. 1974b Studies on statistical characteristics of bubbles by electrical resistivity probe II. *Trans. JSME* **40**, 2302–2310.

SEKOGUCHI, K. 1982 Characteristics of gas–liquid two-phase flow, *Basic Principles and Applications of Multiphase Flow* (Edited by K. Akagawa), p. 83. Japan Science Council.

SERIZAWA, A. 1974 Fluid Dynamic Characteristics of Two-Phase Flow, Ph.D Thesis, Kyoto Univ.

SERIZAWA, A., KATAOKA, I. & MICHIYOSHI, I. 1975a Turbulence structure of air-water bubbly flow I. Measuring techniques. *Int. J. Multiphase Flow* **2**, 221–233.

SERIZAWA, A., KATAOKA, I. & MICHIYOSHI, I. 1975b Turbulence structure of air-water bubbly flow II. Local properties. *Int. J. Multiphase Flow* **2**, 235–246.

SERIZAWA, A., KATAOKA, I. & MICHIYOSHI, I. 1975c Turbulence structure of air-water bubbly flow III. Transport properties. *Int. J. Multiphase Flow* **2**, 247–259.

SERIZAWA, A. 1983 Turbulence structure of bubbly flow, *Flow Characteristics and Applications of Multiphase Flow* (Edited by K. Akagawa), p. 99. Japan Science Council.

TRICE, V. G., JR. & RODGER, W. A. 1956 Light transmittance as a measure of interfacial area in liquid–liquid dispersions. *AIChE J.* **2**(2), 205–210

VETEAU, J. M. 1981 Contribution a L'etude des Techniques de Mesure de L'aire Interfaciale dans les Ecoulements a Bulles, Ph.D. Thesis, L'université Scientifique et Médicale et L'institut National Polytechnique de Grenoble.

VETEAU, J. M. & CHARLOT, R. 1981 Interfacial area measurements in two-phase bubbly flows; comparison between the light attenuation technique and a local method, *European Two-phase Flow Group Meeting*, Eindohoven, June 2–5.

WALLIS, G. B. 1969 *One-Dimensional Two-Phase Flow*, pp. 261–263. McGraw-Hill, New York

ZUBER, N. & FINDLEY, J. A. 1965 Average volumetric concentration in two-phase flow systems. *J. Heat Trans.* **87**, 453–468.

APPENDIX

Derivation of [82]

As shown in [70], $\mathbf{v}_{ij}$ is composed of x, y, and z components $\mathbf{v}_{ixj}$, $\mathbf{v}_{iyj}$, and $\mathbf{v}_{izj}$ which are given by

$$\mathbf{v}_{ixj} = |\mathbf{v}_{ij}| \sin \alpha_j \sin \beta_j \mathbf{n}_x , \qquad [A1]$$

$$\mathbf{v}_{iyj} = |\mathbf{v}_{ij}| \sin \alpha_j \cos \beta_j \mathbf{n}_y , \qquad [A2]$$

$$\mathbf{v}_{izj} = |\mathbf{v}_{ij}| \cos \alpha_j \mathbf{n}_z . \qquad [A3]$$

They should satisfy

$$\mathbf{v}_{ij} = \mathbf{v}_{ixj} + \mathbf{v}_{iyj} + \mathbf{v}_{izj} . \qquad [A4]$$

If there is no preferred direction for an instantaneous transverse velocity, β has a probability density function $h(\beta)$ given by

$$h(\beta) = \frac{1}{2\pi} , \quad 0 < \beta < 2\pi . \qquad [A5]$$

Then in view of [70] with the assumption for $g(\alpha)$ given by [80], one gets

$$\overline{\mathbf{v}_{ix}} = \left(\sum_j \mathbf{v}_{ixj}\right)\Big/\left(\sum_j\right) = \overline{|\mathbf{v}_i|}\int_0^{\pi/2} g(\alpha)\sin\ \alpha\ d\alpha \int_0^{2\pi} h(\beta)\sin\ \beta\ d\beta \cdot n_x = 0\,. \tag{A6}$$

Similarly,

$$\overline{\mathbf{v}_{iy}} = 0\,. \tag{A7}$$

On the other hand,

$$\overline{\mathbf{v}_{iz}} = \overline{|\mathbf{v}_i|}\int_0^{\pi/2} g(\alpha)\cos\ \alpha\ d\alpha \cdot \mathbf{n}_z = \overline{|\mathbf{v}_i|}\frac{\sin\ \alpha_0}{\alpha_0}\mathbf{n}_z\,. \tag{A8}$$

Here no statistical correlations between $|\mathbf{v}_{ij}|$, α, and β have been assumed.

The mean squares of velocity fluctuations are given by the following expressions. For the x components

$$\begin{aligned}\sigma_x^2 \equiv \overline{(\mathbf{v}_{ix} - \overline{\mathbf{v}_{ix}})^2} &= \overline{|\mathbf{v}_{ix}|^2} - \overline{|\mathbf{v}_{ix}|^2} = \overline{|\mathbf{v}_{ix}|^2} \\ &= \overline{|\mathbf{v}_i|^2}\int_0^{\pi/2} g(\alpha)\sin^2\alpha\ d\alpha \int_0^{2\pi} h(\beta)\sin^2\beta\ d\beta \\ &= \frac{1}{2}\overline{|\mathbf{v}_i|^2}\left\{\frac{1}{2} - \frac{1}{4}\frac{\sin\ 2\alpha_0}{\alpha_0}\right\},\end{aligned} \tag{A9}$$

for the y components

$$\sigma_y^2 \equiv \overline{(\mathbf{v}_{iy} - \overline{\mathbf{v}_{iy}})^2} = \overline{|\mathbf{v}_{iy}|^2} = \frac{1}{2}\overline{|\mathbf{v}_i|^2}\left\{\frac{1}{2} - \frac{1}{4}\frac{\sin\ 2\alpha_0}{\alpha_0}\right\} = \sigma_x^2\,, \tag{A10}$$

and for the z components,

$$\begin{aligned}\sigma_z^2 \equiv \overline{(\mathbf{v}_{iz} - \overline{\mathbf{v}_{iz}})^2} &= \overline{|\mathbf{v}_{iz}|^2} - \overline{|\mathbf{v}_{iz}|^2} = \overline{|\mathbf{v}_i|^2}\int_0^{\pi/2} g(\alpha)\cos^2\alpha\ d\alpha - \overline{|\mathbf{v}_{iz}|^2} \\ &= \overline{|\mathbf{v}_i|^2}\left\{\frac{1}{2} + \frac{1}{4}\frac{\sin\ 2\alpha_0}{\alpha_0}\right\} - \overline{|\mathbf{v}_{iz}|^2}\,.\end{aligned} \tag{A11}$$

On the other hand, from [A4], [A6], and [A7],

$$\overline{|\mathbf{v}_i|^2} = \overline{|\mathbf{v}_{ix}|^2} + \overline{|\mathbf{v}_{iy}|^2} + \overline{|\mathbf{v}_{iz}|^2}\,. \tag{A12}$$

Furthermore, from an assumption that the velocity fluctuations are equilateral,

$$\sigma_x^2 = \sigma_y^2 = \sigma_z^2\,. \tag{A13}$$

Then combining the above results given by [A9]–[A13] it can be shown that

$$\frac{\sin\ 2\alpha_0}{2\alpha_0} = \frac{1 - (\sigma_z^2/\overline{|\mathbf{v}_{iz}|^2})}{1 + 3\,(\sigma_z^2/\overline{|\mathbf{v}_{iz}|^2})}\,. \tag{A14}$$